

## **MHD Peristaltic flow of a Jeffrey fluid in an asymmetric channel with partial slip**

**K. Rajanikanth<sup>1</sup>, S. Sreenadh<sup>1</sup>, Y. Rajesh yadav<sup>1</sup> and A. Ebaid<sup>2</sup>**

<sup>1</sup>Department of Mathematics, Sri Venkateswara University, Tirupati 517 502, AP, India

<sup>2</sup>Department of Mathematics, Faculty of Science, Tabuk University, P.O. Box 741, Tabuk 71491, Saudi Arabia

---

### **ABSTRACT**

*In the present note, we have discussed the effects of partial slip on the peristaltic flow of a Jeffrey fluid in an asymmetric channel. The governing equations of motion are simplified using a long wave length approximation. A closed form solution of the momentum equation is obtained by Adomian decomposition method and an exact solution is presented. The expression for pressure rise is calculated using numerical integrations. The graphical results are presented to interpret various physical parameters of interest. The trapping phenomena are also discussed. It is found that the size of the bolus decreases with increasing Hartmann number and Jeffrey material parameter.*

**Key words:** peristaltic; partial slip; Hartmann number; Jeffrey material parameter; shear stress; Adomian decomposition method.

---

### **INTRODUCTION**

The word peristalsis is derived from the Greek word  $\text{περ}\sigma\tau\alpha\lambda\lambda\tau\ell\kappa\omicron\varsigma$ , which means clasping and compressing. It is used to describe a progressive wave of contraction along a channel or tube whose cross-sectional area consequently varies. In physiology, peristalsis is used by the body to propel or mix the contents of a tube as in uretra, gastrointestinal tract, bile ducts and other glandular ducts. Some worms to make locomotion using the mechanism of peristalsis. Roller and finger pumps using viscous fluids also operate on this principle. The principle of peristaltic transport has been exploited for industrial applications like sanitary fluid transport, blood pumps in heart lungs machine and transport of corrosive fluids where the contact of the fluid with the machinery parts is prohibited. Since the first investigation of Latham [1], a number of analytic, numerical and experimental studies of peristaltic flow of different fluids have been reported under different conditions with reference to physiological and mechanical situations. A numerical technique using boundary integral method has been developed by Pozrikidis [2] to investigate peristaltic transport in an asymmetric channel under Stokes flow conditions to understand the fluid dynamics involved. He has studied the streamline patterns and mean flow rate due to different amplitudes and phases of the wall deformation. The existence of trapping regions adjacent to the walls is also observed for some flow rates.

Recently, physiologists observed that the intra uterine fluid flow due to myometrial contractions is peristaltic-type motion and the myometrial contractions may occur in both symmetric and asymmetric directions, De varies *et al.* [3]. Eytan *et al.* [4] have observed that the characterization of non-pregnant woman contractions is very complicated as they are composed of variable amplitudes, a range of frequencies and different wave lengths. It was also observed that the width of the sagittal cross-section of the uterine cavity increases towards the fundus and the cavity is not fully occluded during the contractions. Accordingly, Eytan and Elad [5] have developed a mathematical model of

wall induced peristaltic intra- uterine fluid flow in a two-dimensional channel with wave trains having a phase difference moving independently on the upper and lower walls. These results have been used to evaluate fluid flow pattern in a non-pregnant uterus. They have also calculated the possible particle trajectories to understand the process of embryo transfer before it gets implanted at the uterine-wall. Mishra and Ramachandra Rao [6] discussed the peristaltic transport of a Newtonian fluid in an asymmetric channel. Subba Reddy *et al.* [7] investigated the peristaltic motion of a power-law fluid in an asymmetric channel. Vajravelu *et al.* [8] examined the peristaltic transport of a Casson fluid in contact with a Newtonian fluid in a circular tube with permeable wall. Nadeem [9] discussed the heat transfer in a peristaltic flow of MHD fluid with partial slip. Vajravelu [10] studied the peristaltic transport of a Williamson fluid in asymmetric channel with permeable walls. The flow of MHD fluid with partial slip effects of wall permeability and yield stress on the pumping characteristics have been reported in their investigation.

Due to the flow behavior of non-Newtonian fluids, the governing equations become more complex to handle as additional non-linear terms appear in the equations of motion. There is also no universal constitutive model available which exhibits the characteristics of the all non-Newtonian fluids. Mention may be made to some interesting studies done previously, pertaining to non-Newtonian fluids, which may give insights into their behavior. Some recent studies have been made on the peristaltic motions of conducting, Newtonian and non-Newtonian fluids in asymmetric channels. The MHD flow of a fluid in a channel with elastic, rhythmically contracting walls is of interest in connection with certain problems of the movement of conductive physiological fluids, e.g., the blood and with the need for theoretical research on the operation of a peristaltic MHD compressor. The effect of a moving magnetic field on blood flow was studied by Stud *et al.* [11], and they observed that the effects of a suitable moving magnetic field accelerate the speed of blood. Srivastava and Agarwal [12] considered the blood as an electrically conducting fluid that constitutes a suspension of red cells in the plasma. Mekheimer [13] analyzed the MHD flow of a conducting couple stress fluid in a slit channel with rhythmically contracting walls. Wang *et al.* [14] have studied the MHD peristaltic motion of a Sisko fluid in an asymmetric channel and Kothandapani and Srinivas [15] have examine the peristaltic transport of a Jeffrey fluid under the effect of magnetic field in asymmetric channel with flexible rigid walls. Hayat [16] investigated the effects of an endoscope and magnetic field on the peristalsis involving Jeffrey fluid. In view of these facts, it will be interesting to study the peristaltic flow of conducting Jeffrey fluid flow in a channel bounded by permeable walls.

In the present analysis the fluid considered is of Jeffrey type and is electrically conducting. The Jeffrey model is a relatively simpler linear model using time derivatives instead of convective derivatives and it represents a rheological different from the Newtonian. The main purpose of the present study is to investigate the peristaltic pumping of MHD flow of a Jeffrey fluid in a two-dimensional asymmetric channel having electrically insulated walls. The channel asymmetry is produced by choosing the peristaltic wave train on the walls which have different amplitudes and phase due to the variation in channel width, wave amplitudes and phase differences. The governing equations of fluid flow are solved subject to relevant boundary conditions. The comparison among the three wave forms is also made carefully and the influence of several pertinent parameters on the stream function and pressure drop have been studied and numerical results are presented. The results and discussions presented in this study may be helpful to further understanding MHD peristaltic motion for non-Newtonian fluids in asymmetric channels.

## 2. Mathematical formulation

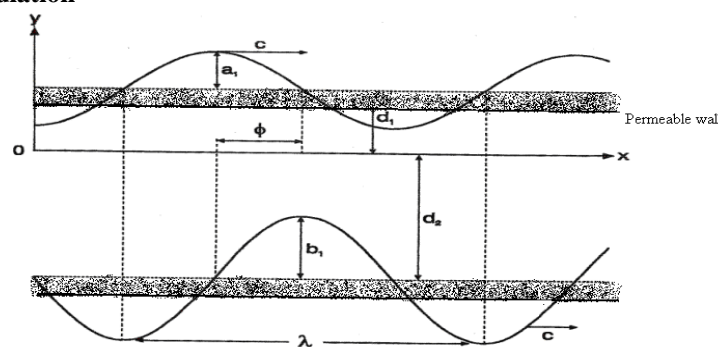


Fig. 1: Schematic diagram of a two-dimensional asymmetric channel

We consider the motion of an incompressible viscous fluid in a two – dimensional channel included by individual wave trains propagating with constant speed  $c$  along the permeable walls of the channel. The wall deformations are given by

$$\bar{h}_1(\bar{X}, \bar{t}) = d_1 + a_1 \cos\left(\frac{2\pi}{\lambda}(\bar{X} - c\bar{t})\right) \dots \text{upper wall}, \quad (1)$$

$$\bar{h}_2(\bar{X}, \bar{t}) = -d_2 - b_1 \cos\left(\frac{2\pi}{\lambda}(\bar{X} - c\bar{t}) + \phi\right) \dots \text{lower wall}, \quad (2)$$

where  $a_1, b_1$  are the amplitude of the waves,  $\lambda$  is the wavelength,  $d_1 + d_2$  (Fig .1) is the width of the channel, the phase difference  $\phi$  varies in the range of  $0 \leq \phi \leq \pi, \phi = 0$ , corresponds to symmetric channel with waves out of phase and  $\phi = \pi$  the waves are in phase and further  $a_1, b_1, d_1, d_2$  and  $\phi$  satisfies the condition

$$a_1^2 + b_1^2 + 2a_1b_1 \cos \phi \leq (d_1^2 + d_2^2)^2. \quad (3)$$

### 3. Equations of motion

The constitutive equations for an incompressible Jeffrey fluid are

$$\bar{T} = -\bar{p} \bar{I} + \bar{S}, \quad (4)$$

$$\bar{S} = \frac{\mu}{1 + \lambda_1} (\bar{\dot{r}} + \lambda_2 \ddot{\bar{r}}) \quad (5)$$

where  $\bar{T}$  and  $\bar{S}$  are Cauchy stress tensor and extra stress tensor, respectively,  $\bar{p}$  is the pressure,  $\bar{I}$  is the identity tensor,  $\lambda_1$  is the ratio of relaxation to retardation times,  $\lambda_2$  is the retardation time  $\dot{\bar{r}}$  is the shear rate and dots over the quantities indicate differentiation with respect to time.

In laboratory frame, the equations governing the two-dimensional motion of an incompressible and the MHD Jeffrey fluid are given as

$$\frac{\partial \bar{U}}{\partial \bar{X}} + \frac{\partial \bar{V}}{\partial \bar{Y}} = 0, \quad (6)$$

$$\rho \left[ \frac{\partial}{\partial t} + \bar{U} \frac{\partial}{\partial \bar{X}} + \bar{V} \frac{\partial}{\partial \bar{Y}} \right] \bar{U} = -\frac{\partial \bar{p}}{\partial \bar{X}} + \frac{\partial (\bar{S}_{\bar{X}\bar{X}})}{\partial \bar{X}} + \frac{\partial (\bar{S}_{\bar{X}\bar{Y}})}{\partial \bar{Y}} - \sigma B_0^2 \bar{U}, \quad (7)$$

$$\rho \left[ \frac{\partial}{\partial t} + \bar{U} \frac{\partial}{\partial \bar{X}} + \bar{V} \frac{\partial}{\partial \bar{Y}} \right] \bar{V} = -\frac{\partial \bar{p}}{\partial \bar{Y}} + \frac{\partial (\bar{S}_{\bar{X}\bar{Y}})}{\partial \bar{X}} + \frac{\partial (\bar{S}_{\bar{Y}\bar{Y}})}{\partial \bar{Y}}. \quad (8)$$

Here,  $\bar{u}, \bar{v}$  are the velocity components in the laboratory frame  $(\bar{X}, \bar{Y})$ ,  $\rho$  is the density,  $\mu$  is the coefficient of viscosity of the fluid,  $\bar{p}$  is the pressure and  $\sigma$  is the electrical conductivity of the fluid. We shall carry out their investigation in a coordinate system moving with the wave speed in which the boundary shape is stationary.

The coordinates and velocities in the laboratory frame  $(\bar{X}, \bar{Y})$  and the wave frame  $(\bar{x}, \bar{y})$  are related by

$$\bar{x} = \bar{X} - ct, \bar{y} = \bar{Y}, \bar{u} = \bar{U} - c, \bar{v} = \bar{V}, \bar{p}(x) = \bar{P}(X, t).$$

where  $\bar{u}, \bar{v}$  are the velocity components in the wave frame,  $\bar{p}$  and  $\bar{P}$  are the pressures in wave and fixed frame of references, respectively. Introducing the following non-dimensional quantities:

$$x = \frac{2\pi \bar{X}}{\lambda}, y = \frac{\bar{Y}}{d_1}, u = \frac{\bar{u}}{c}, v = \frac{\bar{v}}{c\delta}, \delta = \frac{2\pi d_1}{\lambda}, p = \frac{2\pi d_1^2 \bar{P}}{\mu c \lambda}, t = \frac{2\pi c \bar{t}}{\lambda}, h_1 = \frac{\bar{h}_1}{d_1}, h_2 = \frac{\bar{h}_2}{d_1}, \text{Re} = \frac{\rho c d_1}{\mu},$$

$$S = \frac{d_1}{\mu c} \bar{S}, d = \frac{d_2}{d_1}, a = \frac{a_1}{d_1}, b = \frac{b_1}{d_1}.$$

and the stream function

$$u = \frac{\partial \psi}{\partial y}, v = -\delta \frac{\partial \psi}{\partial x}. \quad (9)$$

in Navier–Stokes equations and eliminating the pressure by cross differentiation, we get

$$\delta \text{Re} \left[ \left( \frac{\partial \psi}{\partial y} \frac{\partial}{\partial x} - \frac{\partial \psi}{\partial x} \frac{\partial}{\partial y} \right) \nabla^2 \psi \right] = \left[ \left( \frac{\partial^2}{\partial y^2} - \delta^2 \frac{\partial^2}{\partial x^2} \right) S_{xy} \right] + \delta \left[ \frac{\partial^2}{\partial x \partial y} (S_{xx} - S_{yy}) \right] - M^2 \frac{\partial^2 \psi}{\partial y^2}. \quad (10)$$

in which

$$S_{xx} = \frac{2\delta}{1 + \lambda_1} \left[ 1 + \frac{\delta \lambda_2 c}{d_1} \left( \frac{\partial \psi}{\partial y} \frac{\partial}{\partial x} - \frac{\partial \psi}{\partial x \partial y} \right) \right] \frac{\partial^2 \psi}{\partial x \partial y}, \quad (11)$$

$$S_{xy} = \frac{1}{1 + \lambda_1} \left[ 1 + \frac{\delta \lambda_2 c}{d_1} \left( \frac{\partial \psi}{\partial y} \frac{\partial}{\partial x} - \frac{\partial \psi}{\partial x \partial y} \right) \right] \left( \frac{\partial^2 \psi}{\partial y^2} - \delta^2 \frac{\partial^2 \psi}{\partial x^2} \right), \quad (12)$$

$$S_{yy} = -\frac{2\delta}{1 + \lambda_1} \left[ 1 + \frac{\delta \lambda_2 c}{d_1} \left( \frac{\partial \psi}{\partial y} \frac{\partial}{\partial x} - \frac{\partial \psi}{\partial x \partial y} \right) \right] \frac{\partial^2 \psi}{\partial x \partial y}, \quad (13)$$

$$\nabla^2 = \left( \delta^2 \frac{\partial^2 \psi}{\partial x^2} + \frac{\partial^2 \psi}{\partial y^2} \right),$$

where  $M = \sqrt{\frac{\sigma}{\mu}} B_0 d_1$  is the Hartmann number. Using the long wave length approximation and neglecting the wave

number along with low-Reynolds number, we can find from Eqs. (10) - (13) that

$$\frac{\partial^2}{\partial y^2} \left[ \frac{1}{1 + \lambda_1^2} \frac{\partial^2 \psi}{\partial y^2} \right] - M^2 \frac{\partial^2 \psi}{\partial y^2} = 0. \quad (14)$$

The dimensionless boundary conditions are (Ref. [9])

$$\psi = \frac{q}{2}, \text{ at } y = h_1 = 1 + a \cos 2\pi x, \quad (15)$$

$$\psi = -\frac{q}{2}, \text{ at } y = h_2 = -d - b \cos(2\pi x + \phi), \quad (16)$$

$$\frac{\partial \psi}{\partial y} + \beta \frac{\partial^2 \psi}{\partial y^2} = -1, \text{ at } y = h_1, \quad (17)$$

$$\frac{\partial \psi}{\partial y} - \beta \frac{\partial^2 \psi}{\partial y^2} = -1, \text{ at } y = h_2. \quad (18)$$

where  $q$  is the flux and  $\beta$  is the partial slip parameter and  $a$ ,  $b$ ,  $\phi$  and  $d$  satisfy the relation

$$a^2 + b^2 + 2ab \cos \phi \leq (1 + d)^2.$$

#### 4. Solution of the problem

In order to apply the Adomian decomposition method, Eq. (14) can be written as

$$L\psi = N(\psi_m)_{yy}, \quad (19)$$

where  $N^2 = M^2(1 + \lambda_1)$  and  $L = \frac{d^4}{dy^4}$ . Since a fourth-order difference operator,  $L^{-1}$  is a fourth-fold integration operator

defined by

$$L^{-1} = \int_0^y \int_0^\tau \int_0^\eta \int_0^\xi (\cdot) d\xi d\eta d\tau dy. \quad (20)$$

Operating with  $L^{-1}$  on Eq. (19), yields

$$\psi = c_1 + c_2 y + c_3 \frac{y^2}{2!} + c_4 \frac{y^3}{3!} + NL^{-1}(\psi_m)_{yy}. \quad (21)$$

in which the functions  $C_i(x)$  ( $i=1$  to 4) can be determined by utilizing the boundary conditions (15)- (18).

On applying the standard Adomian decomposition method, one can write

$$\psi = \sum_{m=0}^{\infty} \psi_m. \quad (22)$$

where the components  $\psi_m, m \geq 0$ , will be determined recursively. The following recursively relation is obtained from Eqs. (20)- (21)

$$\psi_0 = c_1 + c_2 y + c_3 \frac{y^2}{2!} + c_4 \frac{y^3}{3!} \quad (23)$$

$$\psi_{m+1} = L^{-1} N(\psi_m)_{yy}, \quad m \geq 0. \quad (24)$$

Hence

$$\begin{aligned} \psi_1 &= \frac{1}{N^3} c_3 \frac{(Ny)^4}{4!} + \frac{1}{N^4} c_4 \frac{(Ny)^5}{5!}, \\ \psi_2 &= \frac{1}{N^3} c_3 \frac{(Ny)^6}{6!} + \frac{1}{N^4} c_4 \frac{(Ny)^7}{7!}, \\ &\vdots \\ &\vdots \\ \psi_m &= \frac{1}{N^3} c_3 \frac{(Ny)^{2m+2}}{(2m+2)!} + \frac{1}{N^4} c_4 \frac{(Ny)^{2m+3}}{(2m+3)!}, \quad m \geq 0. \end{aligned}$$

Through Eq. (22) the expression for  $\psi$  is easily seen to have the form

$$\psi = c_1 + c_2 y + \frac{1}{N^3} c_3 (\cosh Ny - 1) + \frac{1}{N^4} c_4 (\sinh Ny - Ny), \quad (25)$$

which may be simplified as

$$\psi = F_1 + F_2 y + F_3 \cosh Ny + F_4 \sinh Ny. \quad (26)$$

The velocity is given by

$$u = F_2 + NF_3 \sinh Ny + NF_4 \cosh Ny. \quad (27)$$

where the values of  $F_1$ - $F_4$  can be found by using the boundary conditions (15)-(18) and are given by

$$\begin{aligned} F_1 &= \frac{q}{2} + \frac{Nq h_1 \cosh N\left(\frac{h_1-h_2}{2}\right) + \left[ (2 + N^2 q \beta) h_1 - (q + h_1 - h_2) \right] \sinh N\left(\frac{h_1-h_2}{2}\right)}{\left[ 2 - N^2 \beta (h_1 - h_2) \right] \sinh N\left(\frac{h_1-h_2}{2}\right) - N(h_1 - h_2) \cosh N\left(\frac{h_1-h_2}{2}\right)}, \\ F_2 &= - \frac{\left[ (2 + N^2 q \beta) \sinh N\left(\frac{h_1-h_2}{2}\right) + Nq \cosh N\left(\frac{h_1-h_2}{2}\right) \right]}{\left[ (2 - N^2 \beta (h_1 - h_2)) \sinh N\left(\frac{h_1-h_2}{2}\right) \right] - N(h_1 - h_2) \cosh N\left(\frac{h_1-h_2}{2}\right)}, \\ F_3 &= - \frac{\left[ (q + h_1 - h_2) \sinh N\left(\frac{h_1+h_2}{2}\right) \right]}{\left[ 2 - N^2 \beta (h_1 - h_2) \right] \sinh N\left(\frac{h_1-h_2}{2}\right) - N(h_1 - h_2) \cosh N\left(\frac{h_1-h_2}{2}\right)}, \\ F_4 &= \frac{(q + h_1 - h_2) \cosh N\left(\frac{h_1+h_2}{2}\right)}{\left[ 2 - N^2 \beta (h_1 - h_2) \right] \sinh N\left(\frac{h_1-h_2}{2}\right) - N(h_1 - h_2) \cosh N\left(\frac{h_1-h_2}{2}\right)}. \end{aligned}$$

The flux at any axial station in the fixed frame is

$$Q = \int_{h_2}^{h_1} \left( \frac{\partial \psi}{\partial y} + 1 \right) dy = h_1 - h_2 + q, \quad (28)$$

The average volume flow rate over one period of the peristaltic wave is defined as

$$\bar{Q} = \frac{1}{T} \int_0^T Q dt = \frac{1}{T} \int_0^T (q + h_1 - h_2) dt = q + 1 + d \quad (29)$$

The pressure gradient is obtained from the dimensionless momentum equation for the axial velocity as

$$\frac{\partial p}{\partial x} = \frac{N^3}{1 + \lambda_1} \left[ \frac{(q + h_1 - h_2) \cosh N \frac{(h_1 - h_2)}{2}}{\left[ 2 - N^2 \beta (h_1 - h_2) \right] \sinh N \frac{(h_1 - h_2)}{2} - N (h_1 - h_2) \cosh N \frac{(h_1 - h_2)}{2}} \right] \quad (30)$$

The non-dimensional expression for the pressure rise  $\Delta P_\lambda$  is given as follows

$$\Delta P_\lambda = \int_0^{2\pi} \left( \frac{\partial p}{\partial x} \right) dx \quad (31)$$

The non-dimensional shear stress at the upper wall of the channel reduces to

$$S_{xy} = \frac{1}{1 + \lambda_1} \frac{\partial^2 \psi}{\partial y^2} = \frac{1}{1 + \lambda_1} \left[ \frac{N^2 (q + h_1 - h_2) \left[ \left( \sinh N \left( \frac{h_1 + h_2}{2} \right) \cosh Ny + \cosh n \left( \frac{h_1 + h_2}{2} \right) \sinh Ny \right) \right]}{\left[ 2 - N^2 (h_1 - h_2) \beta \right] \sinh N \left( \frac{h_1 - h_2}{2} \right) - N (h_1 - h_2) \cosh N \left( \frac{h_1 - h_2}{2} \right)} \right] \quad (32)$$

The frictional forces, at  $y = h_1$  and  $y = h_2$  denoted by  $F_{\lambda 1}$  and  $F_{\lambda 2}$  respectively are given as follows

$$F_{\lambda 1} = \int_0^1 -h_1^2 \left( \frac{dp}{dx} \right) dx, \quad (33)$$

$$F_{\lambda 2} = \int_0^1 -h_2^2 \left( \frac{dp}{dx} \right) dx. \quad (34)$$

## 6. Expressions for wave shape:

The non-dimensional expressions for the five considered wave forms are given by the following equations:

I. Sinusoidal wave:

$$h_1(x) = 1 + a \sin(x), \quad (35)$$

$$h_2(x) = -d - b \sin(x + \phi), \quad (36)$$

II. Triangular wave:

$$h_1(x) = 1 + a \left\{ \frac{8}{\pi^3} \sum_{m=1}^{\infty} \frac{(-1)^{m+1}}{(2m-1)^2} \sin[(2m-1)x] \right\}, \quad (37)$$

$$h_2(x) = -d - b \left\{ \frac{8}{\pi^3} \sum_{m=1}^{\infty} \frac{(-1)^{m+1}}{(2m-1)^2} \sin[(2m-1)x + \phi] \right\}, \quad (38)$$

III. Square wave:

$$h_1(x) = 1 + a \left\{ \frac{4}{\pi} \sum_{m=1}^{\infty} \frac{(-1)^{m+1}}{(2m-1)} \cos[(2m-1)x] \right\}, \quad (39)$$

$$h_2(x) = -d - b \left\{ \frac{4}{\pi} \sum_{m=1}^{\infty} \frac{(-1)^{m+1}}{(2m-1)} \cos[(2m-1)x + \phi] \right\}, \quad (40)$$

IV. Trapezoidal wave:

$$h_1(x) = 1 + a \left\{ \frac{32}{\pi^2} \sum_{m=1}^{\infty} \frac{\sin \frac{\pi}{8} (2m-1)}{(2m-1)^2} \sin[(2m-1)x] \right\}, \quad (41)$$

$$h_2(x) = -d - b \left\{ \frac{32}{\pi^2} \sum_{m=1}^{\infty} \frac{\sin \frac{\pi}{8} (2m-1)}{(2m-1)^2} \sin[(2m-1)x + \phi] \right\}. \quad (42)$$

## RESULTS AND DISCUSSION

In this section results are presented and discussed for different physical quantities of interest. In Fig. 2, the axial velocity distribution is shown for different parameters partial slip  $\beta$ , Hartmann number  $M$  and Jeffrey material parameter  $\lambda_1$ . From Fig. 2(a) we observed that the increase in the partial slip  $\beta$  decreases the magnitude of the velocity at the middle of the channel and increases at the walls. Figs. 2(b)-2(c) shows the influence of the Hartmann number  $M$  and Jeffrey material parameter  $\lambda_1$  on the axial velocity. It is found that the magnitude of the axial velocity decreases in the center and increases nearer at the walls of the channel with increasing the Hartmann number  $M$  and Jeffrey material parameter  $\lambda_1$ . Fig.3 is plotted to see the effect of the parameters  $\beta$ ,  $M$  and  $\lambda_1$  on the pressure gradient. Figs. 3(a) and 3(c) show that the pressure gradient  $dp/dx$  decreases with increasing the partial slip parameter  $\beta$  and Jeffrey material parameter  $\lambda_1$ , on the other hand, in the wider part of the channel  $x \in [0, 0.3]$  and  $x \in [0.6, 1]$  the pressure gradient is really small, that is, the flow can easily pass without imposition of a large pressure gradient. Besides, in a narrow part of the channel  $x \in [0.3, 0.6]$  a much pressure gradient is required to maintain the  $\beta$  and  $\lambda_1$ , it especially near  $x=0.4$ . Fig. 3(b) indicates that the pressure gradient  $dp/dx$  increases with increasing Hartmann number  $M$  and the maximum pressure gradient is also near  $x=0.4$ .

The pressure rise is important physical measure in the peristaltic mechanism. Fig.4 is a graph of the dimensionless pressure drop versus the dimensionless flow rate  $\bar{Q}$ . The pumping regions are peristaltic pumping ( $\bar{Q} > 0$  and  $\Delta P_\lambda > 0$ ), augment pumping ( $\bar{Q} > 0$  and  $\Delta P_\lambda < 0$ ) and retrograde pumping ( $\bar{Q} < 0$  and  $\Delta P_\lambda > 0$ ). Figs. 4(a) and 4(c) show the effects of the partial slip parameter  $\beta$  and Jeffrey parameter  $\lambda_1$  on  $\Delta P_\lambda$  versus  $\bar{Q}$ . It can be seen that for the adverse pressure gradient ( $\Delta P_\lambda > 0$ ) and free pumping ( $\Delta P_\lambda = 0$ ), the pumping decreases when the values of  $\beta$  and  $\lambda_1$  increase. However, in copumping, the pumping increase with the increase of both parameters,  $\beta$  and  $\lambda_1$ . The effect of Hartmann number  $M$  on pumping characteristics is plotted in Fig. 4(b). It can be seen that for the adverse pressure gradient ( $\Delta P_\lambda > 0$ ) and free pumping ( $\Delta P_\lambda = 0$ ), the pumping increases as the values of  $M$  increase. However, in the copumping region, the pumping decreases with increasing Hartmann number  $M$ .

The variation of the axial shear stress  $s_{xy}$  with  $y$  is calculated from Eq. (32) and is shown in Fig.5 for different physical parameters. In Figs. 5(a) and 5(c) we observed that the curves intersect at origin and the axial shear stress  $s_{xy}$  increases with increasing  $\beta$  and  $\lambda_1$  in the upper wall and an opposite behavior is observed in the lower wall of the channel. The relation between the shear stress  $s_{xy}$  and  $y$  at different values the Hartmann number  $M$  is depicted in Fig. 5 (b). We observe that the curves intersect at origin, the shear stress  $s_{xy}$  decreases with increasing the Hartmann number  $M$  in above of the origin and an opposite behavior is observed in the below of the origin and no effect at the walls.

### Trapping phenomena

Another interesting phenomenon in peristaltic motion is the trapping. It is basically the formation of an internally circulating bolus of fluid by closed stream lines. The trapped bolus will be pushed ahead along the peristaltic waves. The stream lines are calculated from Eq. (26) and plotted in Fig. 6 for various values of  $\beta$ . It is concluded that the volume of the trapping bolus increases with increasing  $\beta$ . The stream lines are drawn in Figs. 7-8 for different values of Hartmann number  $M$  and Jeffrey material parameter  $\lambda_1$ . It is found that the volume of the trapping bolus decreases with increasing Hartmann number  $M$  and Jeffrey material parameter  $\lambda_1$  the bolus disappears for  $M=3$  and  $\lambda_1=2$ . Figs. 9-10 compare various Jeffrey material parameters  $\lambda_1$  for different wave forms like sinusoidal wave, triangular wave, trapezoidal wave and square wave.

## CONCLUSION

In the present note, we have discussed the MHD Peristaltic flow of a Jeffrey fluid in an asymmetric channel with partial slip  $\beta$ . The governing two-dimensional equations have been modeled and then simplified using the long wave length approximation. The results are discussed through graphs. We have concluded the following observations:

- The magnitude of the velocity field increases near the walls and decreases at the center of the channel with increasing  $M$  and  $\lambda_1$ .
- The pressure gradient increases with increasing  $M$ , and decreasing in  $\lambda_1$  and  $\beta$ .
- In the peristaltic pumping region the pressure rise increases with the increase of  $M$ , and decreases with the increase in  $\beta$  and  $\lambda_1$ .

- The shear stress distribution increases in the upper wall and decreases in the lower wall with increasing in both  $\beta$  and  $\lambda_1$ .
- The size of the trapping bolus increases by increasing  $\beta$  and decreases by increasing  $M$  and  $\lambda_1$ , while the bolus disappear at  $M=3$  and  $\lambda_1=2$ .

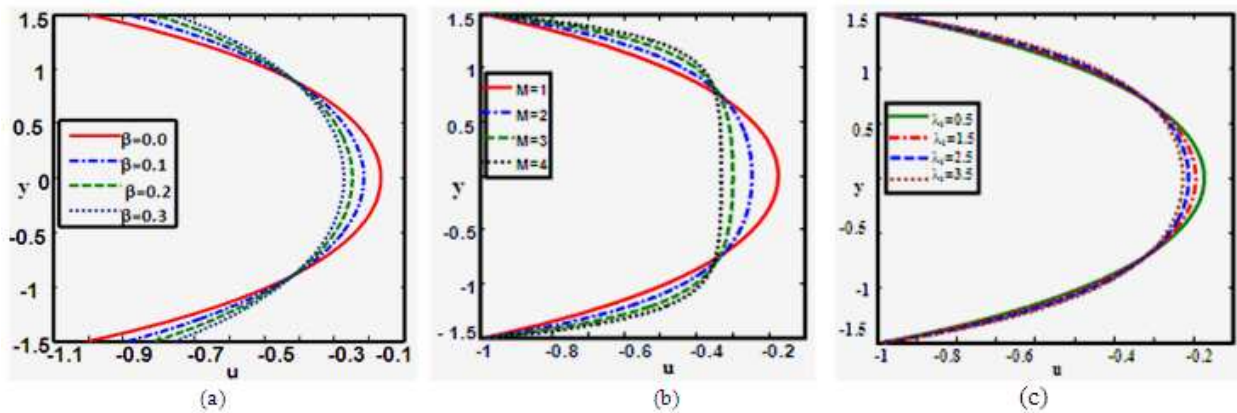


Fig. 2: The velocity profiles with  $a=0.5, b=0.5, d=1.25, x=1, \phi = \pi/3, \bar{Q}=1$ ; (a)  $\lambda_1 = 1$  and  $M=1$ ; (b)  $\beta=0.01, \lambda_1 = 1$  and (c)  $M=1, \beta=0.01$ .

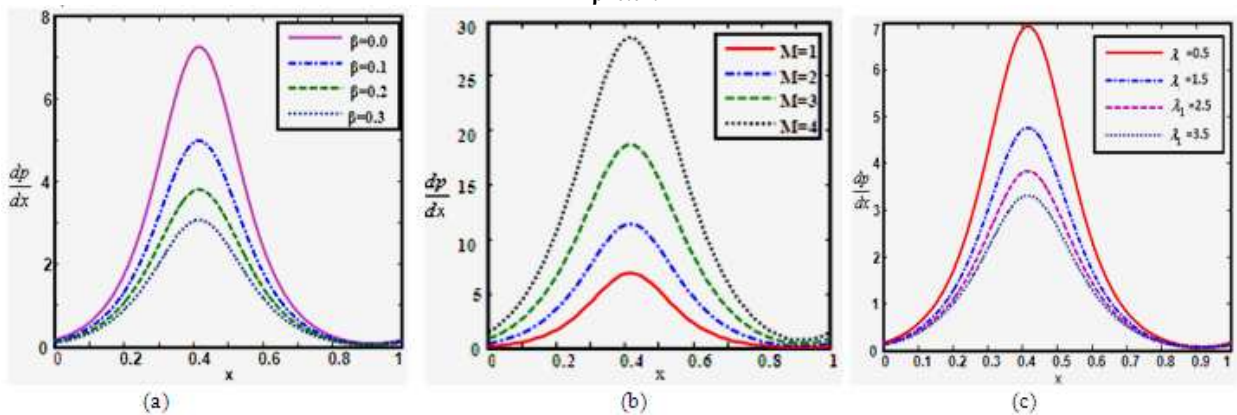


Fig. 3: Distributions of the pressure gradient with  $a=0.5, b=0.5, d=1.25, \phi = \pi/3, \bar{Q} = 1$ ; (a)  $\lambda_1 = 1$  and  $M=1$ ; (b)  $\beta=0.01, \lambda_1 = 1$  and (c)  $M=1, \beta=0.01$ .

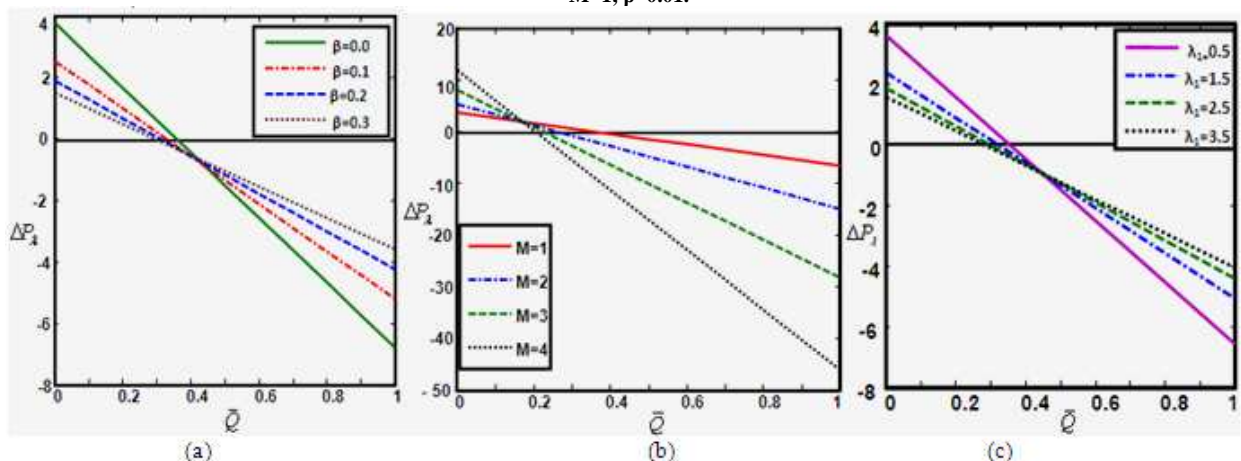


Fig. 4: Effect of the dimensionless flow rate  $\bar{Q}$  on variation of  $\Delta P_\lambda$  with  $a=0.5, b=0.5, d=1.25, \phi = \pi/3$ ; (a)  $\lambda_1 = 0.5, M=1$ ; (b)  $\beta=0.01, M=1$  and (c)  $\beta=0.01, \lambda_1 = 0.5$

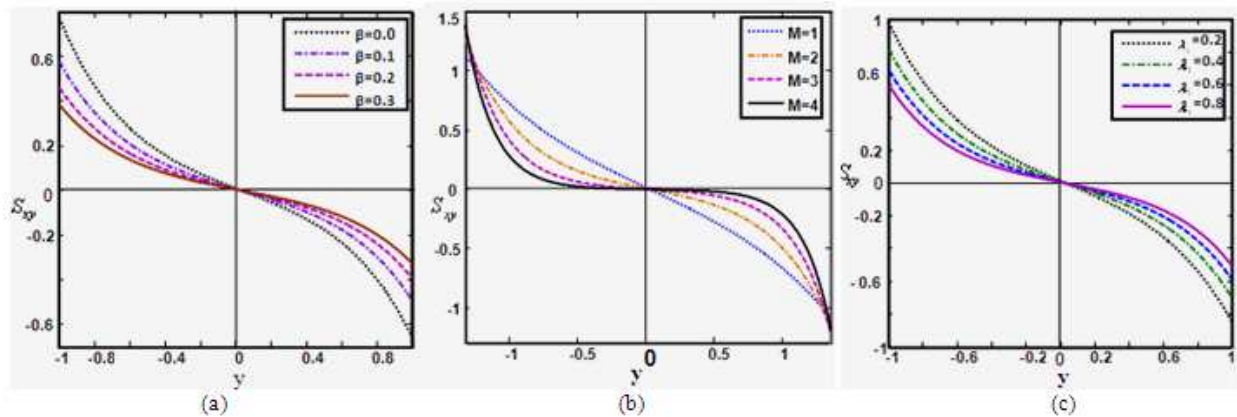


Fig. 5: The axial shear stress distributions at the walls with  $a=0.5, b=0.5, d=1, \phi = \pi/6, \bar{Q}=2$ ; (a)  $\lambda_1=0.5$  and  $M=2$ ; (b)  $\lambda_1=0.5$  and  $\beta=0.1$  and (c)  $M=2$  and  $\beta=0.1$ .

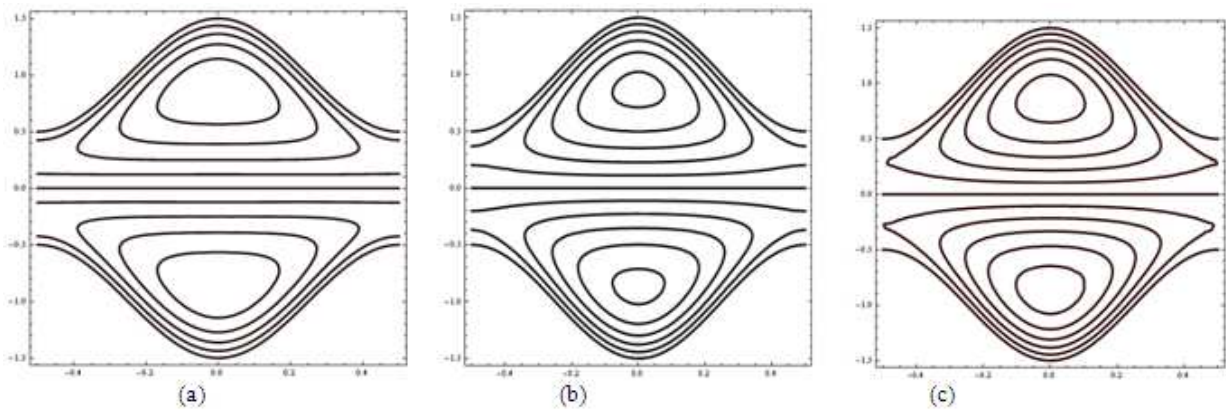


Fig. 6: Streamlines in the wave frame for pumping with  $a=0.5, b=0.5, d=1, \phi=0, \bar{Q}=2, \lambda_1=0.1, M=0.5$ ; (a)  $\beta=0.0$ ; (b)  $\beta=0.1$  and (c)  $\beta=0.2$

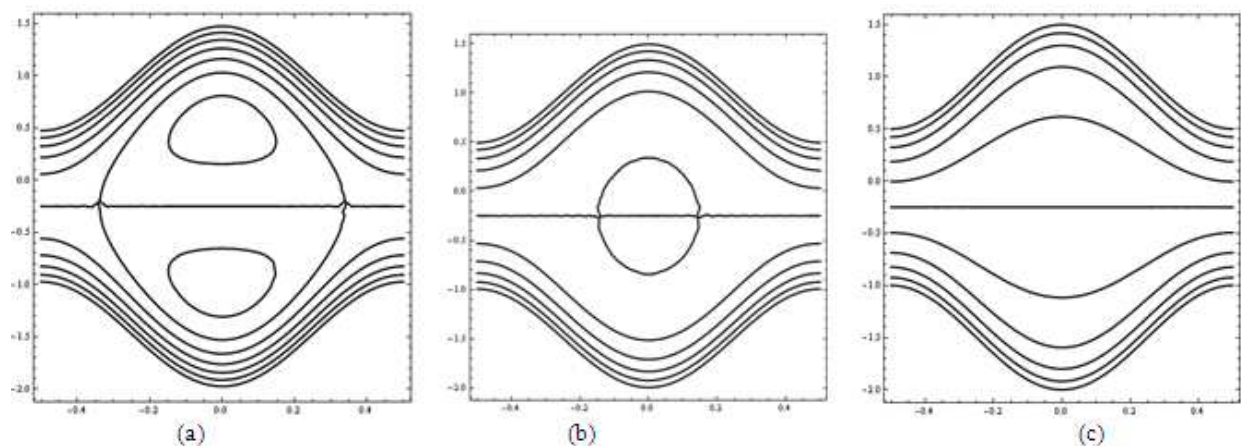


Fig. 7: Streamlines in the wave frame for pumping with  $a=0.5, b=0.5, d=1.5, \phi=0; \lambda_1=1, \beta=0.1, \bar{Q}=1$ ; (a)  $M=1$ ; (b)  $M=2$  and (c)  $M=3$ .

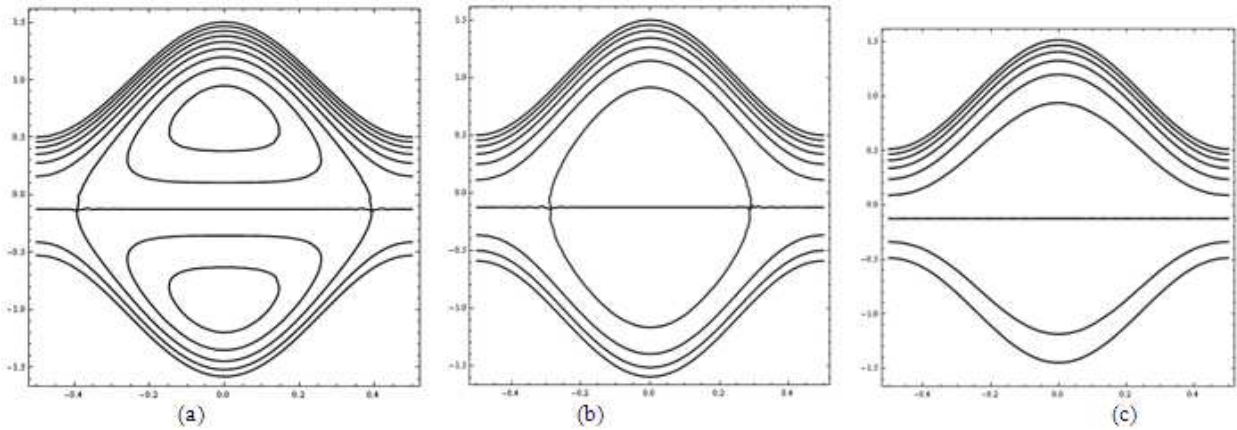


Fig. 8: Streamlines in the wave frame for pumping with  $a=0.5, b=0.5, d=1.25, \phi = 0, \beta=0.1, \bar{Q} = 1, M=2$ ; (a)  $\lambda_1 = 0.1$  (b)  $\lambda_1 = 1$  and (c)  $\lambda_1 = 2$

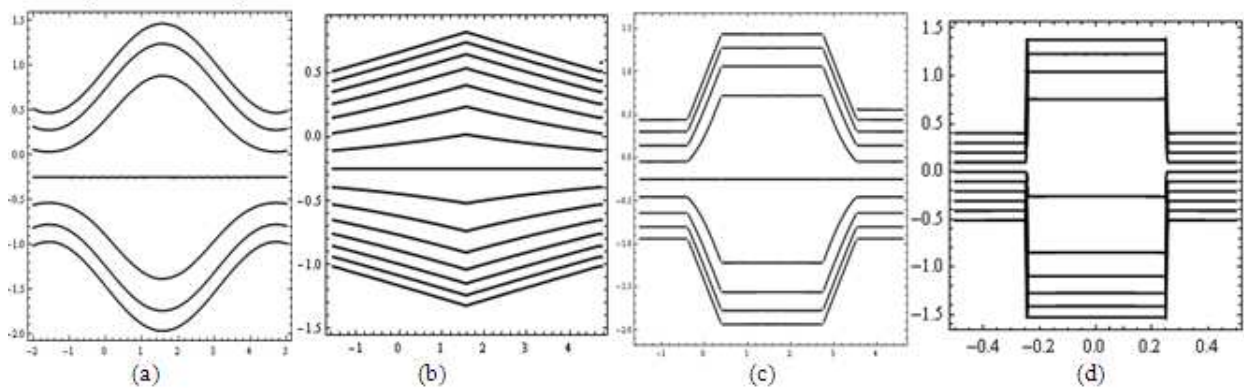


Fig. 9: Streamlines for  $a=0.5, M=1, b=0.5, d=1, \phi = 0, \bar{Q} = 1; \lambda_1 = 0, \beta=0.3$ ; (a) Sinusoidal wave; (b) Triangular wave; (c) Trapezoidal wave and (d) Square wave.

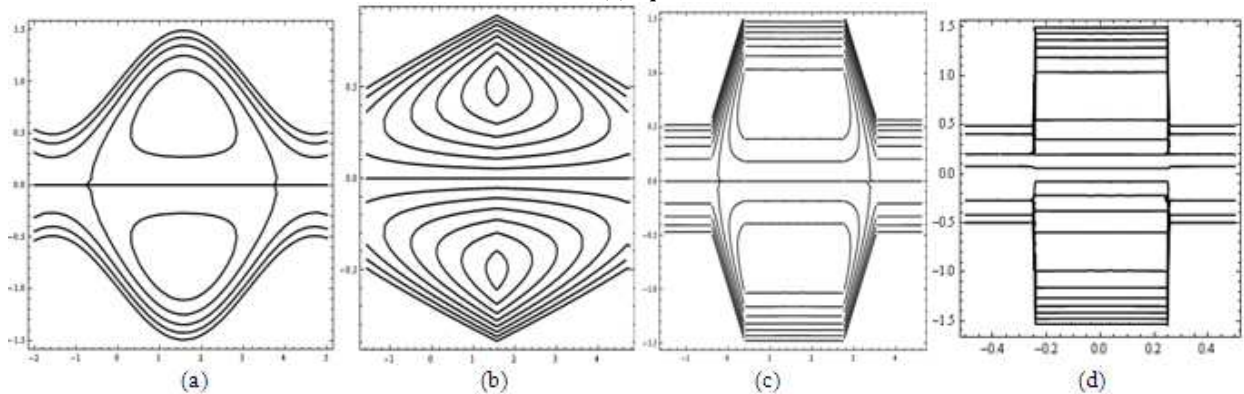


Fig. 10: Streamlines for  $a=0.5, M=1, b=0.5, \phi = 0, d=1, \bar{Q} = 1, \lambda_1 = 1, \beta=0.3$ ; (a) Sinusoidal wave; (b) Triangular wave; (c) Trapezoidal wave and (d) Square wave.

### REFERENCES

- [1]T.W. Latham, Fluid motion in peristaltic pump, M.S. Thesis, MIII, Cambridge, MA, 1966.
- [2]C. Pozrikidis, *J. Fluid Mech.* 180(1987) 515-527.
- [3]K. De varies, EA. Lyons, J. Bavard, CS. Levis and DJ. Lindsay, *Ame. J. Obseterics Gynecol.* 162(1990), 679-682.
- [4]O. Eytan, AJ. Jaffa, J. Har-Toov, E. Dalach, D. Elad, *Ann Biomed Eng.* 27(1999), 372-379.
- [5]O. Eytan, D. Elad, *Bull math Biol.* 61(1999), 221-238.
- [6]M. Mishra, A. Ramachandra Rao, *ZAMP.* 54 (2003), 532-550.

- [7]M.V. Subba Reddy, A. Ramachandra Rao, S. Sreenadh, *Int. J. Non-Linear Mech.* 42(2007), 1153-1161.
- [8]K. Vajravelu, S. Sreenadh, R. Hemadri reddy, K. Murugesan, *International Journal of Fluid Mechanics Research*, Vol. 36(2009)(3), 244-254.
- [9]S. Nadeem, Safia Akram, *Commun Nonlinear Sci Numer Simulat* 15(2010), 312–321.
- [10]K. Vajravelu, S. Sreenadh, K. Rajanikanth, Chanhooon Lee, *Nonlinear Analysis: Real World Applications* 13(2012) , 2804-2822.
- [11]V. K. Stud, G.S. Sephone, R.K.G. Mishra, *Bull. Biol.* 39(1977), 358-390.
- [12]L. M. Srivastava, V. P. Srivastava, *J. Fluid. Mech.* 122(1984), 439-465.
- [13]Kh. S. Mekheimer, *Phys. Lett. A* 371(2008), 4271-4278.
- [14]Y. Wang, T. Hayat, N. Ali, M. Oberlack, *Physica A* 387(2008), 347-362.
- [15]M. Kothandapani, S. Srinivas, *Int. J Non-linear Mech.*43 (2008), 915-924.
- [16]T. Hayat, Niaz Ahmad, N. Ali, Effects of an endoscope and magnetic field on the peristalsis involving Jeffrey fluid, *Communications in Nonlinear Science and Numerical Simulation* 13 (2008), 1581–1591.